Report
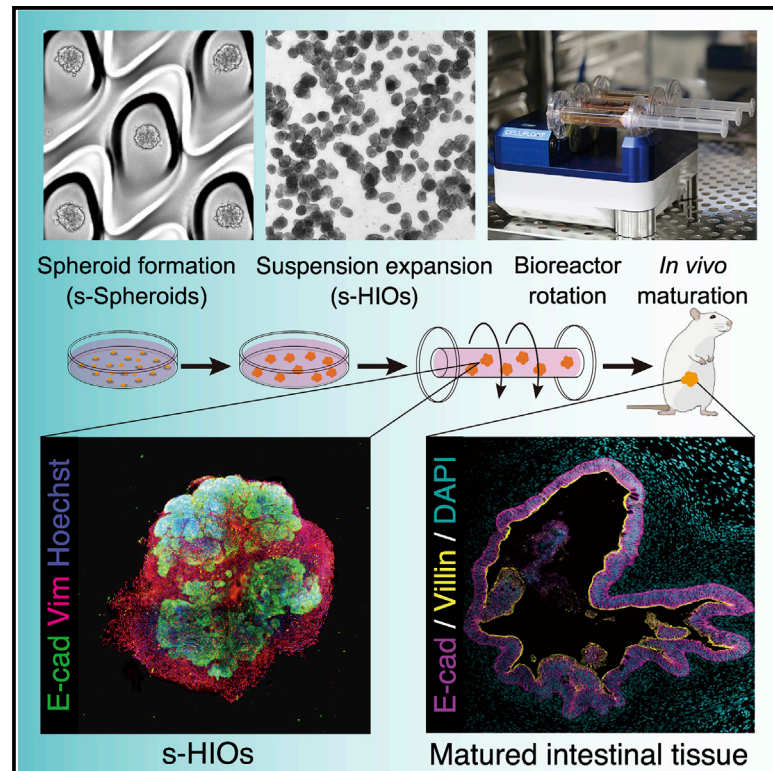
Suspension culture in a rotating bioreactor for efficient generation of human intestinal organoids

Graphical abstract

Highlights

- PSC-derived hindgut cells aggregate into intestinal spheroids in suspension (s-Spheroids)

- s-Spheroids differentiate into suspension-cultured HIOs (s-HIOs)

- Rotational bioreactor accelerates the growth and maturation of s-HIOs

- s-HIOs mature into complex intestinal tissue upon transplantation

Authors

Junichi Takahashi, Tomohiro Mizutani, Hady Yuki Sugihara, ..., Sei Kakinuma, Mamoru Watanabe, Ryuichi Okamoto

Correspondence

tmizutani.gast@tmd.ac.jp

In brief

Takahashi et al. develop a robust differentiation method of spheroids in suspension (s-Spheroids) and an efficient maturation of suspension-cultured human intestinal organoids (s-HIOs) with a rotational bioreactor. s-HIOs further mature into complex intestinal tissue upon transplantation, establishing a reliable culture platform for regenerative medicine.

CellPress

Report

Suspension culture in a rotating bioreactor for efficient generation of human intestinal organoids

Junichi Takahashi,[1] Tomohiro Mizutani,[1,4,*] Hady Yuki Sugihara,[1] Sayaka Nagata,[1] Shu Kato,[1] Yui Hiraguri,[1]
Sayaka Takeoka,[1] Mao Tsuchiya,[1] Reiko Kuno,[1] Sei Kakinuma,[2] Mamoru Watanabe,[3] and Ryuichi Okamoto[1]

[1]Department of Gastroenterology and Hepatology, Tokyo Medical and Dental University (TMDU), 1-5-45 Yushima, Bunkyo-ku, Tokyo
113-8510, Japan
[2]Department of Clinical and Diagnostic Laboratory Science, Tokyo Medical and Dental University (TMDU), 1-5-45 Yushima, Bunkyo-ku,
Tokyo 113-8510, Japan
[3]Advanced Research Institute, Tokyo Medical and Dental University, 1-5-45 Yushima, Bunkyo-ku, Tokyo 113-8510, Japan
[4]Lead contact
*Correspondence: tmizutani.gast@tmd.ac.jp
https://doi.org/10.1016/j.crmeth.2022.100337

MOTIVATION Human intestinal organoids (HIOs) derived from iPSCs hold great promise for regenerative medicine. However, the conventional method employs manual pick up of liberated free-floating hindgut spheroids, resulting in variability in their yield and cell composition. Furthermore, it has been difficult to cultivate large HIOs due to spatial constraints and limited gas/medium exchange of three-dimensional culture. We developed a robust differentiation and maturation protocol of HIOs completely in suspension, which circumvents these limitations.

SUMMARY

Human intestinal organoids (HIOs) derived from human pluripotent stem cells (hPSCs) hold great promise for translational medical applications. A common method to obtain HIOs has been to harvest floating hindgut spheroids arising from hPSCs. As this technique is elegant but burdensome due to the complex protocol and line-to-line variability, a more feasible method is desired. Here, we establish a robust differentiation method into suspension-cultured HIOs (s-HIOs) by seeding dissociated cells on a spheroid-forming plate. This protocol realizes the reliable generation of size-controllable spheroids. Under optimized conditions in a rotating bioreactor, the generated spheroids quickly grow and mature into large s-HIOs with supporting mesenchyme. Upon mesenteric transplantation, s-HIOs further mature and develop complex tissue architecture *in vivo*. This method demonstrates that intestinal tissue can be generated from iPSC-derived HIOs via suspension induction and bioreactor maturation, establishing a reliable culture platform with wide applications in regenerative medicine.

INTRODUCTION

The intestinal tract is a complex organ with absorptive, secretory, and mechanical properties, creating a major hurdle for previous attempts to recreate it *in vitro*.[1] However, as research on hPSCs and adult stem cells (ASCs) have progressed, several approaches to creating human intestinal tissue have been developed in the last decade. One approach is to establish primary intestinal epithelial organoids from the human gut.[2,3] This technology enables the culture of intestinal epithelial stem cells derived from a human donor; however, ASC-derived organoids lack mesenchymal components, which indicates that functionally complex intestinal tissues cannot be recapitulated solely by ASC-derived organoids. This somewhat limits the clinical applicability of the intestinal organoid transplantation, although

it provides a promising source of intestinal epithelial components for direct transplantation.[4–7] Another way to manufacture human intestinal tissue *in vitro* is to induce it from hPSCs. This was achieved by combining hPSC differentiation techniques with the established intestinal epithelial organoid culture method. Human intestinal organoids (HIOs) were differentiated from human induced pluripotent stem cells (iPSCs) with robust and elegant induction through hindgut spheroids by adding several signal transduction factors.[8,9] Human iPSC-based therapy holds great promise for the field of regenerative medicine specifically in its application in organ creation and autologous transplantation.[10] However, the conventional method employs manual pick up of liberated free-floating hindgut spheroids from iPSC monolayer cultures,[8,9,11–14] and pre-conditioning and cellular density of hPSCs is critical for correct differentiation.[15] Owing to the
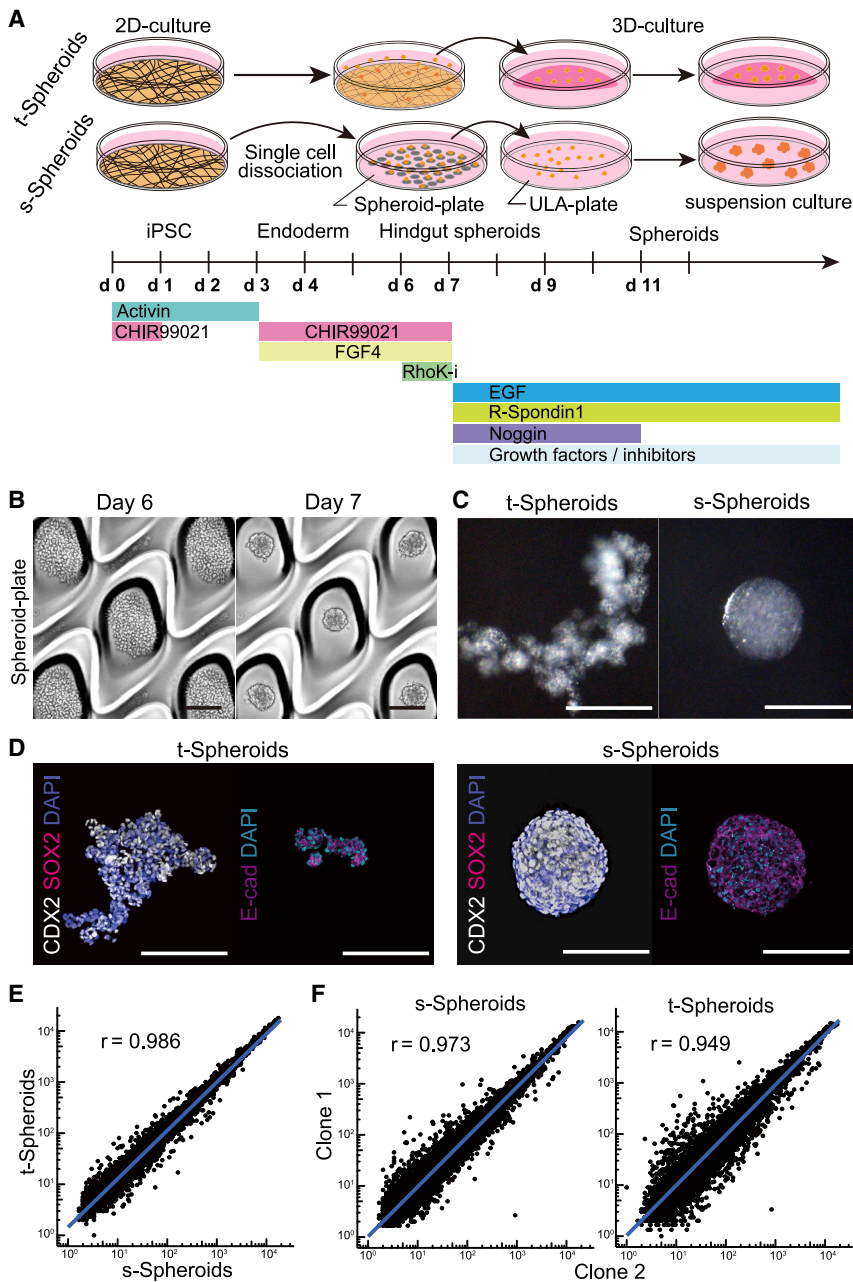
Figure 1. Generation of suspension intestinal spheroids from human iPSCs

(A) Schematic differentiation protocol of t-Spheroids and s-Spheroids from human iPSCs.

(B) Bright-field images of hindgut-induced cells forming spheroids in the microwells. Scale bar, 200 μm.

(C and D) Bright-field images (C) and whole-mount immunostaining of CDX2, SOX2, and E-cadherin (E-cad) (D) of s-Spheroids and t-Spheroids. Scale bars, 200 μm.

(E and F) Scatterplots of microarray data depicting gene-expression variation between t-Spheroids and s-Spheroids (E) and two iPSC lines (clones 1 and 2) in s-Spheroids (left panel) and t-Spheroids (right panel) (F) Blue solid lines are fitted linear regression. r is the percentage-bend correlation coefficient.

an optimized culture protocol for the growth and maturation of floating HIOs. We employ a variety of designed ultra-low attachment culture plates and cell number variety to induce uniform, efficient, and size-adjustable HIOs in suspension. Then, we demonstrate that induced HIOs mature in suspension culture using a rotating bioreactor and establish an optimized culture condition to generate intestinal tissue by *in vivo* transplantation.

RESULTS

Differentiation of human intestinal spheroids in suspension

First, to induce the spheroids in suspension, we utilized the previously reported induction condition of spheroids[8,9,15] and modified them to the suspension culture condition (Figure 1A). We employed EZSPHERE/EZ-BindShut spheroid-forming plates, which have many microwells coated with ultra-low attachment (ULA) polymer.[18–21] To adapt the previous condition to a suspension induction, hindgut cells were dissociated into single cells and seeded onto these plates on day 6. Seeded cells were cultured for 24 h, quickly fusing and forming uniform-sized spheroids in the microwells of the plates (Figure 1B; Videos S1 and S2). This aggregation method proved equally effective using hindgut cells differentiated from multiple iPSC lines, confirming the robustness of this protocol (Figure S1A). In contrast to traditional spheroids (t-Spheroids), which are detached fragments of induced cells, our method produced spherical aggregations, which we termed suspension spheroids (s-Spheroids) (Figure 1C). To confirm that s-Spheroids were induced into intestinal spheroids, the expression of *CDX2*, a hindgut marker, was examined by quantitative reverse transcription

nuances of this protocol, formed hindgut spheroids have diverse cellular heterogeneity and differentiation potential through the induction process, which leads to sizable variations in cellular composition among induced HIOs.[12,16] For example, smaller free-floating spheroids tend to fail further maturation into HIOs. Furthermore, the amount and size of generated spheroids differ greatly between iPSC lines.[17] Therefore, the development of a simpler and more robust protocol for obtaining homogeneous spheroids and mature HIOs would provide a solid foundational basis for future clinical applications.

Here, we establish a robust suspension differentiation method of human iPSCs into intestinal spheroids and present

PCR (qRT-PCR). *CDX2* expression in s-Spheroids did not differ significantly from that in t-Spheroids in two independent iPSC lines, suggesting that s-Spheroids keep the directed differentiation toward intestinal lineages (Figure S1B). Next, whole-mount immunostaining was performed to confirm its expression and cell distribution. The induced spheroids expressed CDX2 and E-cadherin but not a foregut marker SOX2, confirming their differentiation into hindgut spheroids. However, s-Spheroids showed a more homogeneous expression pattern of CDX2 throughout the spheroids compared with the mottled expression pattern observed in t-Spheroids (Figure 1D), suggesting that the induction method of s-Spheroids has led to a more homogeneous cell population. To confirm that s-Spheroids and t-Spheroids share transcriptional similarity, the gene expression at the time of spheroid generation was analyzed by microarray analysis. As expected, both generated spheroids showed significant similarity ($r = 0.986$), indicating that the level of induction as well as the resulting spheroids are consistent across both conditions (Figure 1E). Moreover, to check the difference among iPSC lines, we compared the gene expressions between two independent clones in both induction methods. Consistent with the data, gene-expression levels were almost identical ($r = 0.973$) between two clones in s-Spheroid induction, but more variation in gene expression was observed in the t-Spheroid induction method ($r = 0.949$) (Figure 1F). By constructing percentile bootstrap confidence intervals, we found that s-Spheroid correlation was significantly higher than that of t-Spheroid ($p < 0.0001$). Taken together, these data suggest that our induction method for suspension-intestinal spheroids has a more robust differentiation process regardless of the cell line's differentiation propensity.

### Designing the size of s-Spheroids on suspension plates

As we confirmed that dissociated cells aggregate to form floating spheroids, we further attempted to design the size of spheroids by selecting the size of the microwell. To that end, dissociated induced cells were seeded onto three variations of specially designed EZSPHERE SP plates (microwell diameters: 300, 500, and 1,400 μm) and EZ-BindShut 96 well plate (diameter: $-6,500$ μm). As expected, the formed spheroid size was affected by microwell diameter (Figure 2A). While the size of t-Spheroids varied from 50 to 300 μm, reflecting random pick up, all three variations of EZSPHERE plates produced uniformly sized s-Spheroids typically within 100 μm diameter in range (Figure 2B). Then, we attempted to extend this technique to design the diameter of the spheroids by varying the number of the seeded cells on the EZ-BindShut 96-well plate. There was a clear correlation between the number of seeded cells and the diameter of the resulting spheroids (Figure 2C; Video S3). This result suggested that the size of the spheroids can be controlled by elucidating the correlation between the number of seeded cells and the diameter of the formed spheroids. To assess the exact size of the formed spheroids, we employed a high-throughput bright-field imaging scanner, Cell3 iMager duos, to analyze the size of spheroids (Figures S2A and S2B). The diameter of the spheroids followed a semi-logarithmic pattern in relation to seeded cell number (Figure 2D). Varying spheroid sizes had little effect on differentiation trajectory, as indicated by comparable *CDX2* expressions (Figure S3A).

However, when seeded cells exceeded 4×10^5, they aggregated into a biconcave disk-like structure as opposed to a sphere (Figure S3B). Henceforth, s-Spheroids were produced with 1×10^5 cells as a balance between ease of handling and size. Given the long-standing limitation of conventional spheroid formation, namely lack of spheroid size control and size heterogeneity,[12,22] our robust method to generate scalable uniform-sized spheroids has a promising application in regenerative medicine.

For culturing the generated spheroids, we developed a suspension culture method to overcome the spatial limitation inherent in the conventional Matrigel-embedding method (Figure S3C). To this end, Matrigel, a key extracellular matrix for conventional culture of t-Spheroids, was added to the medium. The optimum concentration for s-Spheroid culture was investigated (0%, 3%, 5%, 10%, 20%, and 100%). As expected, the formed spheroids could not be maintained in a Matrigel-free medium. Cultured spheroids showed thinner cystic features in 3%–5% Matrigel medium, and above 10% Matrigel medium, the spheroids showed extensive budding organoid structures surrounded by mesenchyme, like t-Spheroids (Figure S3D). Of the compared concentrations, 10% Matrigel provided the best results for maintaining and handling s-Spheroids. Then, we examined the optimal growth factor combination for suspension culture. First, we employed previously reported intestine growth medium (ENR), consisting of epidermal growth factor (EGF), Noggin, and R-spondin1, for three-dimensional maturation of spheroids, but the medium was found unsuitable for maintaining floating spheroids for long-term culture. Based on the previous report that activation of BMP signaling elicits stable posterior gut induction,[11] we started culture medium optimization with Noggin-withdrawal (E(N)R) as a foundation. After referring to various previous reports[2,23] and examining various culture factors (Table S1), we confirmed that the addition of A83-01, a transforming growth factor β (TGF-β) receptor inhibitor, or the combination of insulin-like growth factor 1 (IGF-1) and fibroblast growth factor 2 (FGF-2) resulted in enhanced growth (Figures 2E and 2F). Accordingly, qRT-PCR analysis showed that *CDX2* and *PDX1* expressions, proximal small-intestine markers,[24] were increased when A83-01 (E(N)RA) or IGF-1/FGF-2 (E(N)RIFA) was added to the medium. When it pertains to *SOX2*, a foregut endoderm marker, E(N)RA medium resulted in minimized expression across the examined conditions (Figure 2G). We then examined the long-term effect of E(N)RA and E(N)RIFA culture conditions on the specification of posterior gut endoderm in s-Spheroids. In line with the trend observed in RNA expression, spheroids treated with E(N)RIFA showed scattered SOX2 expression in whole-mount immunostaining, in contrast to the spheroid in E(N)RA condition, which showed no expression of SOX2 (Figure 2H). Therefore, we concluded that the addition of A83-01 could increase the size of s-Spheroids while preserving the directed differentiation toward small intestinal cell types.

Suspension culture in a rotating bioreactor accelerates spheroid growth and maturation

So far, we have established an optimized induction protocol and the ability to control spheroid size; however, maintaining larger
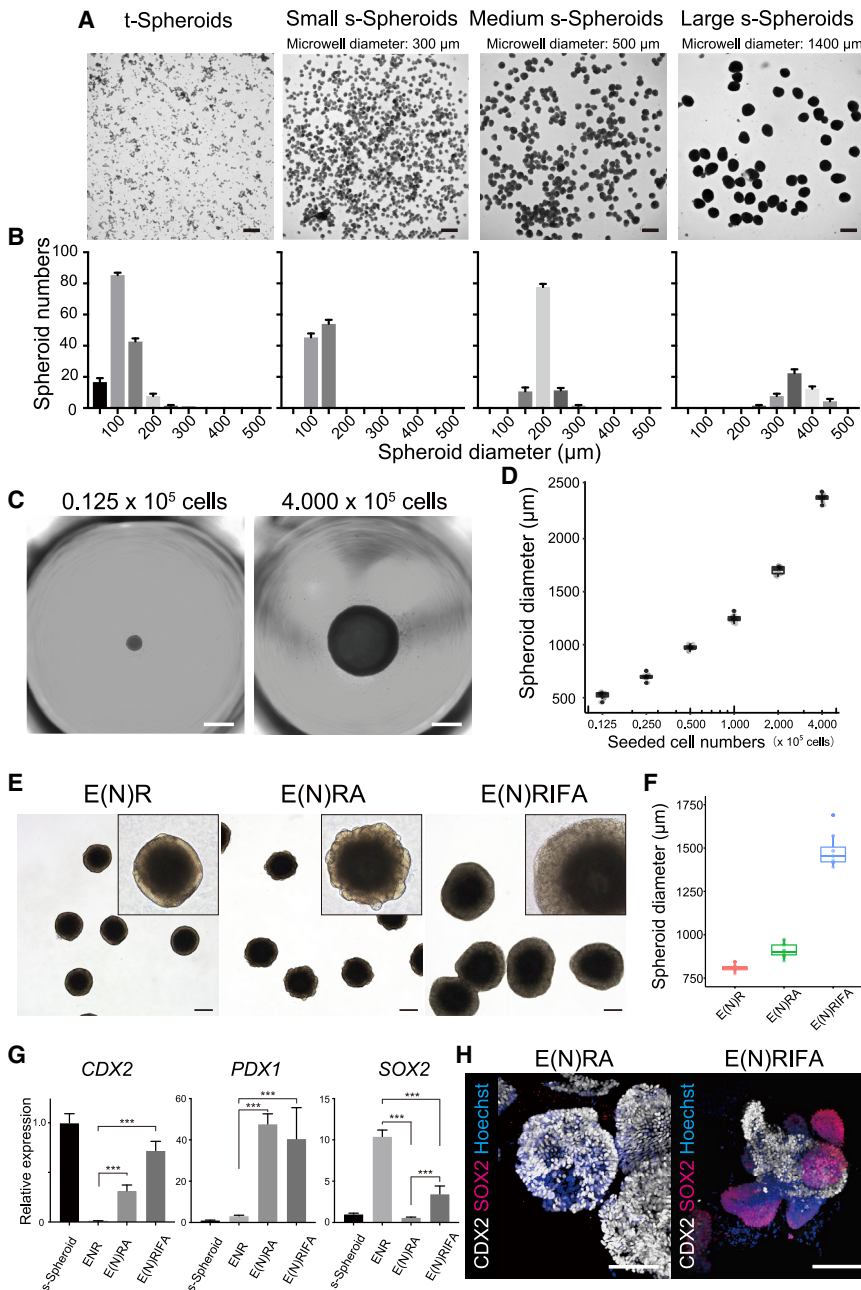
Figure 2. s-Spheroid size design and stable culture condition in suspension

(A) Bright-field images of small, medium, and large spheroids formed in microwell diameters: 300, 500, and 1,400 μm, respectively. Scale bar, 500 μm.

(B) Diameter quantification of spheroids formed in each microwell condition compared with t-Spheroids. Data are means ± SD for triplicate independent experiments.

(C) Bright-field images depicting formed s-Spheroids by seeding indicated cell numbers. Scale bar, 1,000 μm.

(D) The relation between seeded cell numbers and formed s-Spheroid diameter.

(E) Bright-field images of s-Spheroids cultured under the indicated conditions with high-magnification inset at top right. Scale bar, 500 μm.

(F) Diameter quantification of s-Spheroids cultured in each condition.

(G) Expression analyses of *CDX2*, *PDX1*, and *SOX2* in s-Spheroids cultured in each indicated condition (day 10) relative to expressions at s-Spheroid formation. Bars are means ± SD for triplicate independent experiments. Student's t test (***$p < 0.0001$).

(H) Whole-mount immunostaining of CDX2 and SOX2 in s-Spheroids cultured in E(N)RA and E(N)RIFA conditions. Scale bar, 200 μm.

led to the centralization of spheroids, resulting in increased spheroid fusion (Figure S3F). Thus, the bioreactor proved more suitable for dynamic suspension culture. In this bioreactor, constant rotation of a cylindrical vessel filled with culture medium creates a flow within the vessel, allowing the spheroids to continuously float. Spheroids in static suspension were gradually damaged, and the growth rate was decreased in the later phases of the culture. In contrast, the rotated spheroids showed dramatic growth in the bioreactor during culture (Figure 3C). To assess the exact growth speed of the cultured spheroids, we quantified the size and numbers of the spheroids with Cell3 iMager duos. Consistent with the observation, s-

spheroids in suspension proved quite difficult (Figure S3E), likely due to the diffusional limitations in bioactive molecule, nutrient, and gas exchange.[22] Therefore, we attempted to cultivate s-Spheroids in a rotating bioreactor and compared them with static suspension condition (Figure 3A). First, we generated spheroids from seeded induced cells and transferred them to ULA plates to culture for 3 days to solidify the directed differentiation. Then, spheroids were transferred to a bioreactor cell culture system (CELLFLOAT CellPet 3D-iPS) and cultured in a suspended rotating state (Figure 3B). Note that a common orbital shaker (bioSan) was trialed; however, the circular motion

Spheroids in the bioreactor grew without stalling for 4 weeks. When placed in the bioreactor, spheroids formed epithelial structures surrounded by mesenchyme-like traditional HIOs (t-HIOs) and thus were termed suspension-cultured HIOs (s-HIOs). Comparing the spheroids cultured in the bioreactor with those in static suspension culture, their diameters gradually increased after shrinking in the first few days. The spheroids in rotating suspension culture grew at an accelerated rate, significantly outsizing those grown in static suspension (Figure 3D).

To confirm whether the rotated organoids had the same properties as t-HIOs,[8] we performed tissue analysis by
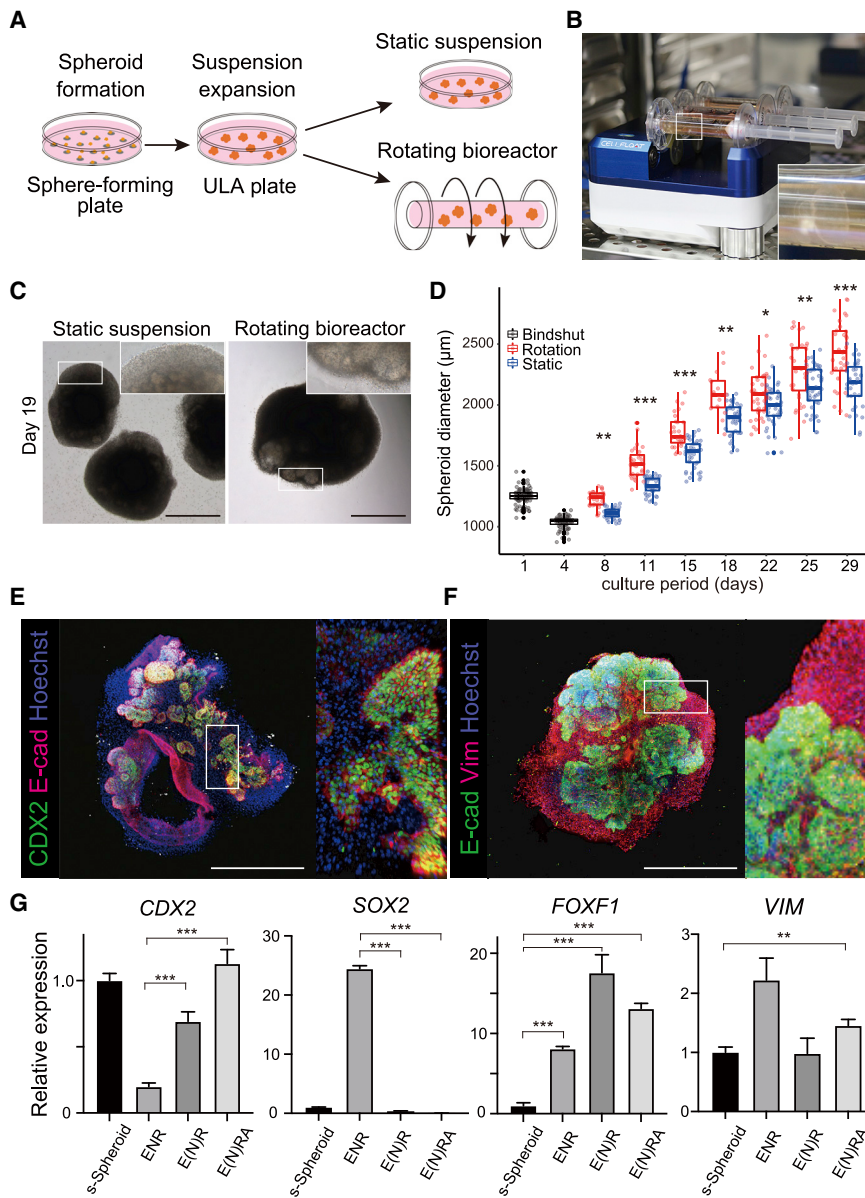
Figure 3. Rotational culture in a bioreactor accelerates the growth and maturation of suspension HIOs

(A) Schematic representation of suspension spheroid culture system encompassing static suspension and rotating suspension in a bioreactor.

(B) Image showing the rotating bioreactor composed of 10 mL culture vessels on bioreactor. Spheroids float in the culture vessel (inset).

(C) Bright-field images of s-Spheroids cultured in both conditions, static suspension and rotating bioreactor, on day 19. Both showed mesenchymal growth surrounding spheroids (inset). Scale bars, 1,000 μm.

(D) Growth rates of s-Spheroids in two culture conditions (static and rotation suspensions). The black boxes represent generated spheroid sizes on days 1 and 4 (Bindshut). False discovery rate (FDR)-adjusted t test (*p < 0.01, **p < 0.001, ***p < 0.0001).

(E and F) Whole-mount immunostaining of CDX2, E-cad, and Hoechst (E) and VIM, E-cad, and Hoechst (F) in s-HIOs cultured in rotational suspension with high-magnification inset at right. Scale bars, 1,000 μm.

(G) Expression analyses of *CDX2*, *SOX2*, *FOXF1*, and *VIM* in s-HIOs cultured in rotational suspension in each medium condition (day 30) relative to expressions at s-Spheroid formation. Bars are means ± SD for triplicate independent experiments. Student's t test (**p < 0.001, ***p < 0.0001).

dimensional culture.[8] It should also be emphasized that FOXF1, a splanchnic mesoderm marker that codevelops and interrelates with definitive endoderm in the fetal foregut,[25] was strongly expressed in s-HIOs, suggesting that coordinated development of endoderm and mesoderm progenitors occurred in the cultured s-HIOs. Taken together, we have demonstrated that rotational suspension culture using a bioreactor enables the growth, maintenance, and maturation of large s-HIOs, which is more beneficial as a basis for translational medicine compared with conventional HIO culture methods.

immunohistochemistry, which showed that s-HIOs consist of CDX2/E-cadherin double-positive intestinal epithelial cells surrounded by a vimentin-positive mesenchymal layer (Figures 3E and 3F). This was also confirmed with mRNA expression analysis of cultured organoids. s-HIOs cultured in E(N)RA maintained comparable *CDX2* and *SOX2* expression to s-Spheroids but had greater expressions of vimentin and forkhead box F1 (*FOXF1*), well-known mesenchymal markers in HIO,[8,17,25] suggesting that the suspension culture in the rotating bioreactor promotes not only the efficient growth of s-Spheroids but also their maturation to s-HIOs, likely through the improved exchange of culture factors and gases (Figure 3G). The fact that s-HIOs were surrounded by vimentin (VIM)-expressing mesenchyme suggests that the rotational floating culture condition is suitable for the maturation of HIOs to the same extent as t-HIOs in three-

Engrafted s-HIO matured into human intestinal tissue

We decided to confirm further maturation of s-HIOs by *in vivo* transplantation into immunocompromised non-obese diabetic severe combined immunodeficiency (NOD/SCID) interleukin-2 receptor gamma chain (IL2Rγ)^{null} (NSG) mice. A recent study illustrated the mouse mesentery as a more physiologic and anatomic engraftment site for HIO transplantation than a subcutaneous region or kidney capsule.[26–28] To determine which site was optimal for the maturation of large s-HIOs, we performed mesenteric and subcutaneous organoid transplantations into NSG mice and allowed the engrafted HIOs to mature *in vivo* for
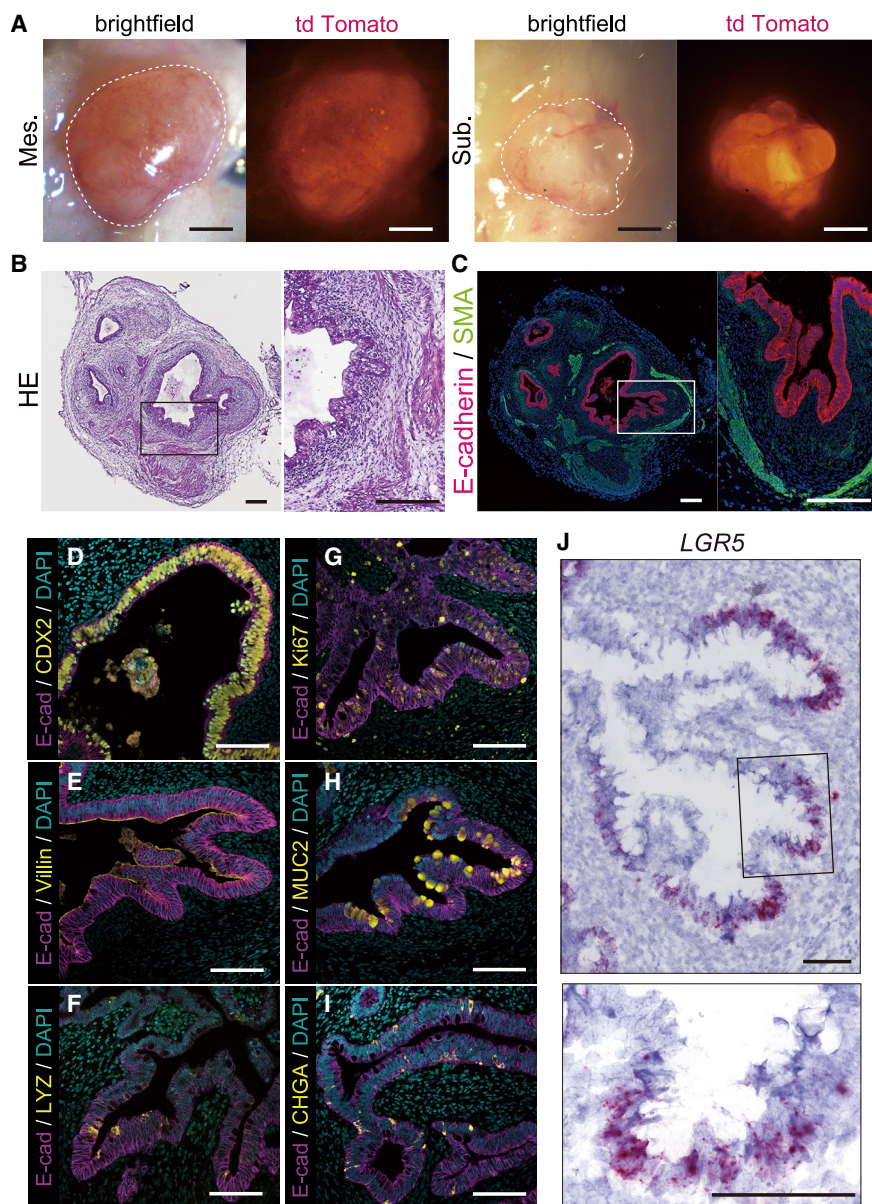
Figure 4. s-HIOs cultured in rotational suspension engraft to mature into intestinal tissue *in vivo*

(A) Bright-field and fluorescent images (tdTomato) of engrafted s-HIOs in the mesentery (Mes.) and subcutaneous lesion (Sub.) of NSG mice, outlined in white. Scale bars, 1 mm.

(B and C) H&E staining (B) and E-cad/SMA immunostaining (C) of engrafted s-HIOs. Scale bars, 200 μm.

(D–I) Immunostaining of CDX2 (D), villin (E), lysozyme (F), Ki67 (G), MUC2 (H), and ChgA (I) in E-cad-positive epithelial cell layer of engrafted s-HIOs. Scale bars, 100 μm.

(J) *In situ* hybridization of *LGR5* in engrafted s-HIOs. Scale bars, 100 μm.

ence of all the small intestinal epithelial cell lineages, including villin-positive enterocytes, mucin 2 (MUC2)-positive goblet cells, lysozyme-positive Paneth cells, and chromogranin A-positive enteroendocrine cells, which confirmed the recapitulation of a functional intestinal tissue (Figures 4D–4I). In contrast, s-HIO-derived epithelial tissue did not express the colonic markers carbonic anhydrase II (CA2), special AT-rich sequence-binding protein 2 (SATB2), or colonic-type goblet cell marker MUC5B, suggesting that their small intestinal regional identity was maintained after transplantation (Figures S4C–S4E). Finally, we performed leucine-rich-repeat-containing G-protein-coupled receptor 5 (*LGR5*) *in situ* hybridization to determine whether engrafted intestinal tissue maintains intestinal stem cells like previous reports.[9,29] We found that *LGR5* mRNA-signal-labeled cells were present within the engrafted HIOs and localized to epithelial cells at the base of the crypt-like structures in the engraftment (Figure 4J). These data demon-

4 weeks. At the time of harvest, engrafted HIOs grew larger with surrounding mesenchymal structure at both grafting sites (Figures 4A and S4A). Between graft sites, mesenteric grafts grew twice as large as subcutaneous grafts in diameter (Figure S4B). This reaffirmed the mesentery as a more physiological and optimal transplantation site for large s-HIOs.

Histological analyses of mesentery-engrafted s-HIOs confirmed that an E-cadherin-positive single intestinal epithelial cell layer was constructed in the transplanted organoids, part of which formed crypt-like invaginated structures resembling matured intestinal tissue. The intestinal epithelial structure was surrounded by a mesenchymal layer and alpha-smooth muscle actin (SMA)-positive smooth muscle layers (Figures 4B and 4C). Further immunostaining analyses of the intestinal epithelial cell layer showed the pres-

strate that large s-HIOs cultured in the rotating bioreactor have the potential to differentiate into mature intestinal tissue upon transplantation.

DISCUSSION

In this study, we successfully developed a robust suspension induction method for the generation of hindgut spheroids by using ULA spheroid-forming plates and established an efficient suspension culture condition with a rotating bioreactor. As the previously reported method was to induce and collect hindgut spheroids manually,[8,15] the resulting spheroids lacked uniformity in size and cell composition. Our method achieved faster and more robust induction of homogeneous intestinal

spheroids in suspended culture. Coincidentally, two recent publications have introduced their own improvements on the conventional method. One induces hindgut spheroids from dissociated single cells in suspension, similar to our method, but requires three-dimensional culture for subsequent maturation.[17] The other reports suspension culture of HIOs; however, the induction of hindgut spheroids, which is the most complicated and variable part, follows the conventional method.[30] Our study demonstrates effective suspension culture throughout the entire culture process from hindgut spheroid induction to HIO maturation.

For suspension culture, we found that low concentrations of Matrigel were required, agreeing with the recent report on ASC-derived organoids.[31] We also found that the addition of A83-01 accelerated the growth of s-Spheroids while maintaining the hindgut identity. A83-01 is reported to support colonic epithelial cell renewal and is used in ASC-derived HIO culture.[2,32] Recently, TGF-β inhibition was reported to induce the cell-cycle reentry of dormant colonic epithelial stem cells,[33] suggesting a possible mechanism for the size increase in s-HIOs. Thus, we demonstrated that our suspension culture method supports comparable maturation to the established three-dimensional culture.

To realize the potential of this spheroid-forming system, we introduced a rotating bioreactor known to be beneficial when culturing large tissues owing to improved growth factor and gas transfer. As expected, spheroids cultured in the rotating bioreactor grew larger than in a static condition. Importantly, the spheroids maintained in the bioreactor matured into s-HIOs *in vitro*. Cultured organoids developed a VIM-positive mesenchymal layer, which is an established hallmark of matured HIOs.[8,9] These results confirmed that s-HIOs are comparable to reported t-HIOs. However, it remains to be examined whether the presence of mechanical stimuli like exposure to shear stress, which is expected in the bioreactor system, affected the maturation and growth of s-HIOs. Since this culture method is entirely in suspension, it simplifies much of the culture protocols, even ridding the need for serial passaging. The ease of culture and scale-up potential of our method will be highly beneficial in advancing iPSC-based translational medicine.

For further examination of the quality of HIO produced with our method, we transplanted matured s-HIOs into immunodeficient mice to achieve further structural and cellular maturation *in vivo*. Finally, we performed immunostaining and *in situ* hybridization to confirm that the s-HIOs grown *in vitro* were constructing intestinal tissue *in vivo*. We observed all the small intestinal cell types including LGR5-positive stem cells in the engrafted tissue, indicating that suspension cultured HIOs using the rotating bioreactor are able to mature into human small intestinal tissue upon transplantation. These results highlight the great potential for *in vivo* applications of suspension HIOs matured in size and complexity in a rotating bioreactor.

Intriguingly, by further optimizing the culture conditions of HIOs or by coculturing with other cell populations, attempts to develop HIOs into a more complex culture system capable of recapitulating various patho-physiological and developmental processes have recently been reported.[16,34,35] For example, endogenous endothelial cells residing in HIOs were expanded in a specific culture condition to form self-vascularization.[16] Moreover, by combining hPSC-derived neural crest cells and induced HIOs, human intestinal tissue containing a functional enteric nervous system was generated.[34] Such attempts to construct more complex intestinal tissues by modular assembly have been made using t-HIO. As the suspension HIO protocol presented here allows for easy assembly of other cell types, it is expected that reported cocultures can be easily implemented in our suspension culture system.

In conclusion, we demonstrated the suspension induction and robust maturation of intestinal organoids differentiated from human iPSCs. As this method enables more efficient and stable induction of HIOs compared with previously reported methods, we believe that our approach will be widely used as an improved method for intestinal spheroid generation with translational and potential long-term clinical applications.

Limitations of the study

As we discussed, t-HIOs have spatial limitations and require passaging in conventional three-dimensional culture, whereas s-HIOs do not. Thus, direct qualitative and quantitative comparisons of t-HIOs and s-HIOs were experimentally difficult and not performed. Although the rotational bioreactor enhanced the growth of HIOs in suspension, the underling mechanism, like enhanced factor exchange or mechanical stimulation, remains to be elucidated. Moreover, the suspension culture we established requires Matrigel, an extracellular matrix (ECM) extracted from mouse sarcoma. For future clinical applications, further modifications to our method are necessary to realize xeno-free culture of s-HIOs.

STAR★METHODS

Detailed methods are provided in the online version of this paper and include the following:

- KEY RESOURCES TABLE
- RESOURCE AVAILABILITY
  - Lead contact
  - Materials availability
  - Data and code availability
- EXPERIMENTAL MODEL AND SUBJECT DETAILS
  - Animals
  - Cell culture of iPSCs
- METHOD DETAILS
  - Differentiation of human iPSCs into intestinal spheroids
  - HIO differentiation in suspension culture
  - HIO differentiation in the three-dimensional culture
  - Culture of suspension HIOs in a rotating bioreactor
  - RNA isolation and qRT-PCR
  - Microarray analysis
  - Immunofluorescent staining of spheroids
  - Immunofluorescent staining of whole-mount spheroids
  - *In situ* hybridization
  - Spheroid transplantation
- QUANTIFICATION AND STATISTICAL ANALYSIS

AUTHOR CONTRIBUTIONS

J.T. and T.M. conceived the idea and designed the experiments; J.T. and T.M. conducted the experiments with assistance from S.N., H.Y.S., S. Kato, Y.H., S.T., R.K., M.T., and S. Kakinuma; J.T., H.Y.S., and T.M. analyzed the results and wrote the manuscript; T.M., M.W., and R.O. supervised the project. All authors contributed to the discussion and interpretation of the results.

DECLARATION OF INTERESTS

The authors declare no competing interest.

REFERENCES

1. Qi, D., Shi, W., Black, A.R., Kuss, M.A., Pang, X., He, Y., Liu, B., and Duan, B. (2020). Repair and regeneration of small intestine: a review of current engineering approaches. Biomaterials 240, 119832. https://doi.org/10.1016/j.biomaterials.2020.119832.

2. Sato, T., Stange, D.E., Ferrante, M., Vries, R.G.J., Van Es, J.H., Van den Brink, S., Van Houdt, W.J., Pronk, A., Van Gorp, J., Siersema, P.D., and Clevers, H. (2011). Long-term expansion of epithelial organoids from human colon, adenoma, adenocarcinoma, and Barrett's epithelium. Gastroenterology 141, 1762–1772. https://doi.org/10.1053/j.gastro.2011.07.050.

3. Jung, P., Sato, T., Merlos-Suárez, A., Barriga, F.M., Iglesias, M., Rossell, D., Auer, H., Gallardo, M., Blasco, M.A., Sancho, E., et al. (2011). Isolation and in vitro expansion of human colonic stem cells. Nat. Med. 17, 1225–1227. https://doi.org/10.1038/nm.2470.

4. Yui, S., Nakamura, T., Sato, T., Nemoto, Y., Mizutani, T., Zheng, X., Ichinose, S., Nagaishi, T., Okamoto, R., Tsuchiya, K., et al. (2012). Functional engraftment of colon epithelium expanded in vitro from a single adult Lgr5+ stem cell. Nat. Med. 18, 618–623. https://doi.org/10.1038/nm.2695.

5. Fukuda, M., Mizutani, T., Mochizuki, W., Matsumoto, T., Nozaki, K., Sakamaki, Y., Ichinose, S., Okada, Y., Tanaka, T., Watanabe, M., and Nakamura, T. (2014). Small intestinal stem cell identity is maintained with functional Paneth cells in heterotopically grafted epithelium onto the colon. Genes Dev. 28, 1752–1757. https://doi.org/10.1101/gad.245233.114.

6. Sugimoto, S., Ohta, Y., Fujii, M., Matano, M., Shimokawa, M., Nanki, K., Date, S., Nishikori, S., Nakazato, Y., Nakamura, T., et al. (2017). Reconstruction of the human colon epithelium in vivo. Cell Stem Cell 22, 171–176.e5. https://doi.org/10.1016/j.stem.2017.11.012.

7. Sugimoto, S., Kobayashi, E., Fujii, M., Ohta, Y., Arai, K., Matano, M., Ishikawa, K., Miyamoto, K., Toshimitsu, K., Takahashi, S., et al. (2021). An organoid-based organ-repurposing approach to treat short bowel syndrome. Nature 592, 99–104. https://doi.org/10.1038/s41586-021-03247-2.

8. Spence, J.R., Mayhew, C.N., Rankin, S.A., Kuhar, M.F., Vallance, J.E., Tolle, K., Hoskins, E.E., Kalinichenko, V.V., Wells, S.I., Zorn, A.M., et al. (2011). Directed differentiation of human pluripotent stem cells into intestinal tissue in vitro. Nature 470, 105–109. https://doi.org/10.1038/nature09691.

9. Watson, C.L., Mahe, M.M., Múnera, J., Howell, J.C., Sundaram, N., Poling, H.M., Schweitzer, J.I., Vallance, J.E., Mayhew, C.N., Sun, Y., et al. (2014). An in vivo model of human small intestine using pluripotent stem cells. Nat. Med. 20, 1310–1314. https://doi.org/10.1038/nm.3737.

10. O'Neill, J.D., Pinezich, M.R., Guenthart, B.A., and Vunjak-Novakovic, G. (2021). Gut bioengineering strategies for regenerative medicine. Am. J. Physiol. Gastrointest. Liver Physiol. 320, G1–G11. https://doi.org/10.1152/ajpgi.00206.2020.

11. Múnera, J.O., Sundaram, N., Rankin, S.A., Hill, D., Watson, C., Mahe, M., Vallance, J.E., Shroyer, N.F., Sinagoga, K.L., Zarzoso-Lacoste, A., et al. (2017). Differentiation of human pluripotent stem cells into colonic organoids via transient activation of BMP signaling. Cell Stem Cell 21, 51–64.e6. https://doi.org/10.1016/j.stem.2017.05.020.

12. Arora, N., Imran Alsous, J., Guggenheim, J.W., Mak, M., Munera, J., Wells, J.M., Kamm, R.D., Asada, H.H., Shvartsman, S.Y., and Griffith, L.G. (2017). A process engineering approach to increase organoid yield. Development 144, 1128–1136. https://doi.org/10.1242/dev.142919.

13. Zhang, R.-R., Koido, M., Tadokoro, T., Ouchi, R., Matsuno, T., Ueno, Y., Sekine, K., Takebe, T., and Taniguchi, H. (2018). Human iPSC-derived posterior gut progenitors are expandable and capable of forming gut and liver organoids. Stem Cell Rep. 10, 780–793. https://doi.org/10.1016/j.stemcr.2018.01.006.

14. Takahashi, Y., Sato, S., Kurashima, Y., Yamamoto, T., Kurokawa, S., Yuki, Y., Takemura, N., Uematsu, S., Lai, C.-Y., Otsu, M., et al. (2018). A refined culture system for human induced pluripotent stem cell-derived intestinal epithelial organoids. Stem Cell Rep. 10, 314–328. https://doi.org/10.1016/j.stemcr.2017.11.004.

15. McCracken, K.W., Howell, J.C., Wells, J.M., and Spence, J.R. (2011). Generating human intestinal tissue from pluripotent stem cells in vitro. Nat. Protoc. 6, 1920–1928. https://doi.org/10.1038/nprot.2011.410.

16. Holloway, E.M., Wu, J.H., Czerwinski, M., Sweet, C.W., Wu, A., Tsai, Y.-H., Huang, S., Stoddard, A.E., Capeling, M.M., Glass, I., and Spence, J.R. (2020). Differentiation of human intestinal organoids with endogenous vascular endothelial cells. Dev. Cell 54, 516–528.e7. https://doi.org/10.1016/j.devcel.2020.07.023.

17. Pitstick, A.L., Poling, H.M., Sundaram, N., Lewis, P.L., Kechele, D.O., Sanchez, J.G., Scott, M.A., Broda, T.R., Helmrath, M.A., Wells, J.M., and Mayhew, C.N. (2022). Aggregation of cryopreserved mid-hindgut endoderm for more reliable and reproducible hPSC-derived small intestinal organoid generation. Stem Cell Rep. 17, 1889–1902. https://doi.org/10.1016/j.stemcr.2022.06.011.

18. Ebert, A.D., Shelley, B.C., Hurley, A.M., Onorati, M., Castiglioni, V., Patitucci, T.N., Svendsen, S.P., Mattis, V.B., McGivern, J.V., Schwab, A.J., et al. (2013). EZ spheres: a stable and expandable culture system for the generation of pre-rosette multipotent stem cells from human ESCs and iPSCs. Stem Cell Res. 10, 417–427. https://doi.org/10.1016/j.scr.2013.01.009.

19. Hosoyama, T., McGivern, J.V., Van Dyke, J.M., Ebert, A.D., and Suzuki, M. (2014). Derivation of myogenic progenitors directly from human pluripotent stem cells using a sphere-based culture. Stem Cells Transl. Med. 3, 564–574. https://doi.org/10.5966/sctm.2013-0143.

20. Zhang, R.-R., Takebe, T., Miyazaki, L., Takayama, M., Koike, H., Kimura, M., Enomura, M., Zheng, Y.-W., Sekine, K., and Taniguchi, H. (2014). Efficient hepatic differentiation of human induced pluripotent stem cells in a

three-dimensional microscale culture. Methods Mol. Biol. *1210*, 131–141. https://doi.org/10.1007/978-1-4939-1435-7_10.

21. Onozato, D., Yamashita, M., Nakanishi, A., Akagawa, T., Kida, Y., Ogawa, I., Hashita, T., Iwao, T., and Matsunaga, T. (2018). Generation of intestinal organoids suitable for pharmacokinetic studies from human induced pluripotent stem cells. Drug Metab. Dispos. *46*, 1572–1580. https://doi.org/10.1124/dmd.118.080374.

22. Velasco, V., Shariati, S.A., and Esfandyarpour, R. (2020). Microtechnology-based methods for organoid models. Microsyst. Nanoeng. *6*, 76. https://doi.org/10.1038/s41378-020-00185-3.

23. Fujii, M., Matano, M., Toshimitsu, K., Takano, A., Mikami, Y., Nishikori, S., Sugimoto, S., and Sato, T. (2018). Human intestinal organoids maintain self-renewal capacity and cellular diversity in niche-inspired culture condition. Cell Stem Cell *23*, 787–793.e6. https://doi.org/10.1016/j.stem.2018.11.016.

24. Sinagoga, K.L., McCauley, H.A., Múnera, J.O., Reynolds, N.A., Enriquez, J.R., Watson, C., Yang, H.-C., Helmrath, M.A., and Wells, J.M. (2018). Deriving functional human enteroendocrine cells from pluripotent stem cells. Development *145*, dev165795. https://doi.org/10.1242/dev.165795.

25. Han, L., Chaturvedi, P., Kishimoto, K., Koike, H., Nasr, T., Iwasawa, K., Giesbrecht, K., Witcher, P.C., Eicher, A., Haines, L., et al. (2020). Single cell transcriptomics identifies a signaling network coordinating endoderm and mesoderm diversification during foregut organogenesis. Nat. Commun. *11*, 4158. https://doi.org/10.1038/s41467-020-17968-x.

26. Cortez, A.R., Poling, H.M., Brown, N.E., Singh, A., Mahe, M.M., and Helmrath, M.A. (2018). Transplantation of human intestinal organoids into the mouse mesentery: a more physiologic and anatomic engraftment site. Surgery *164*, 643–650. https://doi.org/10.1016/j.surg.2018.04.048.

27. Poling, H.M., Wu, D., Brown, N., Baker, M., Hausfeld, T.A., Huynh, N., Chaffron, S., Dunn, J.C.Y., Hogan, S.P., Wells, J.M., et al. (2018). Mechanically induced development and maturation of human intestinal organoids in vivo. Nat. Biomed. Eng. *2*, 429–442. https://doi.org/10.1038/s41551-018-0243-9.

28. Singh, A., Poling, H.M., Sundaram, N., Brown, N., Wells, J.M., and Helmrath, M.A. (2020). Evaluation of transplantation sites for human intestinal organoids. PLoS One *15*, e0237885. https://doi.org/10.1371/journal.pone.0237885.

29. Finkbeiner, S., Hill, D., Altheim, C., Dedhia, P., Taylor, M., Tsai, Y.-H., Chin, A., Mahe, M., Watson, C., Freeman, J., et al. (2015). Transcriptome-wide analysis reveals hallmarks of human intestine development and maturation in vitro and in vivo. Stem Cell Rep. *4*, 1140–1155. https://doi.org/10.1016/j.stemcr.2015.04.010.

30. Capeling, M.M., Huang, S., Childs, C.J., Wu, J.H., Tsai, Y.-H., Wu, A., Garg, N., Holloway, E.M., Sundaram, N., Bouffi, C., et al. (2022). Suspension culture promotes serosal mesothelial development in human intestinal organoids. Cell Rep. *38*, 110379. https://doi.org/10.1016/j.celrep.2022.110379.

31. Hirokawa, Y., Clarke, J., Palmieri, M., Tan, T., Mouradov, D., Li, S., Lin, C., Li, F., Luo, H., Wu, K., et al. (2021). Low-viscosity matrix suspension culture enables scalable analysis of patient-derived organoids and tumoroids from the large intestine. Commun. Biol. *4*, 1067. https://doi.org/10.1038/s42003-021-02607-y.

32. Reynolds, A., Wharton, N., Parris, A., Mitchell, E., Sobolewski, A., Kam, C., Bigwood, L., El Hadi, A., Münsterberg, A., Lewis, M., et al. (2014). Canonical Wnt signals combined with suppressed TGF/BMP pathways promote renewal of the native human colonic epithelium. Gut *63*, 610–621. https://doi.org/10.1136/gutjnl-2012-304067.

33. Ishikawa, K., Sugimoto, S., Oda, M., Fujii, M., Takahashi, S., Ohta, Y., Takano, A., Ishimaru, K., Matano, M., Yoshida, K., et al. (2022). Identification of quiescent LGR5+ stem cells in the human colon. Gastroenterology *163*, 1391–1406.e24. https://doi.org/10.1053/j.gastro.2022.07.081.

34. Workman, M.J., Mahe, M.M., Trisno, S., Poling, H.M., Watson, C.L., Sundaram, N., Chang, C.-F., Schiesser, J., Aubert, P., Stanley, E.G., et al. (2017). Engineered human pluripotent-stem-cell-derived intestinal tissues with a functional enteric nervous system. Nat. Med. *23*, 49–59. https://doi.org/10.1038/nm.4233.

35. Uchida, H., Machida, M., Miura, T., Kawasaki, T., Okazaki, T., Sasaki, K., Sakamoto, S., Ohuchi, N., Kasahara, M., Umezawa, A., and Akutsu, H. (2017). A xenogeneic-free system generating functional human gut organoids from pluripotent stem cells. JCI Insight *2*, e86492. https://doi.org/10.1172/jci.insight.86492.

36. Rousselet, G.A., Pernet, C.R., and Wilcox, R.R. (2021). The percentile bootstrap: a primer with step-by-step instructions in R. Adv. Methods Pract. Psychol. Sci. *4*, 251524592091188. https://doi.org/10.1177/2515245920911881.

37. Fujioka, T., Shimizu, N., Yoshino, K., Miyoshi, H., and Nakamura, Y. (2010). Establishment of induced pluripotent stem cells from human neonatal tissues. Hum. Cell *23*, 113–118. https://doi.org/10.1111/j.1749-0774.2010.00091.x.

38. Masaki, H., Kato-Itoh, M., Umino, A., Sato, H., Hamanaka, S., Kobayashi, T., Yamaguchi, T., Nishimura, K., Ohtaka, M., Nakanishi, M., and Nakauchi, H. (2015). Interspecific in vitro assay for the chimera-forming ability of human pluripotent stem cells. Development *142*, 3222–3230. https://doi.org/10.1242/dev.124016.

39. Mizutani, T., Nakamura, T., Morikawa, R., Fukuda, M., Mochizuki, W., Yamauchi, Y., Nozaki, K., Yui, S., Nemoto, Y., Nagaishi, T., et al. (2012). Real-time analysis of P-glycoprotein-mediated drug transport across primary intestinal epithelium three-dimensionally cultured in vitro. Biochem. Biophys. Res. Commun. *419*, 238–243. https://doi.org/10.1016/j.bbrc.2012.01.155.

40. Dekkers, J.F., Alieva, M., Wellens, L.M., Ariese, H.C.R., Jamieson, P.R., Vonk, A.M., Amatngalim, G.D., Hu, H., Oost, K.C., Snippert, H.J.G., et al. (2019). High-resolution 3D imaging of fixed and cleared organoids. Nat. Protoc. *14*, 1756–1771. https://doi.org/10.1038/s41596-019-0160-8.

41. Wang, F., Flanagan, J., Su, N., Wang, L.-C., Bui, S., Nielson, A., Wu, X., Vo, H.-T., Ma, X.-J., and Luo, Y. (2012). RNAscope A novel in situ RNA analysis platform for formalin-fixed, paraffin-embedded tissues. J. Mol. Diagn. *14*, 22–29. https://doi.org/10.1016/j.jmoldx.2011.08.002.

STAR★METHODS

KEY RESOURCES TABLE

REAGENT or RESOURCE	SOURCE	IDENTIFIER
Antibodies		
CDX2 (1:200)	BioGenex	Cat#MU392A-5U; RRID: AB_2650531
SOX2 (1:500)	Abcam	Cat#ab97959; RRID: AB_2341193
E-cadherin (1:100)	R&D	Cat#AF648; RRID: AB_355504
MUC2 (1:100)	Santa Cruz	Cat#Sc15334; RRID: AB_2146667
MUC5B (1:500)	Novus Biologicals	Cat#NBP1-92151; RRID: AB_11019602
Chromogranin A (1:1000)	DiaSorin	Cat#SP-1
Villin (1:100)	Novus Biologicals	Cat#NBP1-85335; RRID: AB_11020888
Ki67 (1:50)	Novus Biologicals	Cat#NB600-1252; RRID: AB_2142376
alpha-Smooth Muscle Actin (1:150)	Novus Biologicals	Cat#NB600-531; RRID: AB_10000930
Vimentin (1:200)	Novus Biologicals	Cat#NB300-223; RRID: AB_10003206
SATB2 (1:100)	Santa Cruz	Cat#sc81376; RRID: AB_1129287
Lysozyme (1:1000)	Sigma	Cat#HPA048284; RRID: AB_2680339
Carbonic Anhydrase II (1:200)	Sigma	Cat#HPA001550; RRID: AB_1078393
Alexa 488 donkey anti-rabbit IgG (1:200)	Invitrogen	Cat#A21206; RRID: AB_2535792
Alexa 488 donkey anti-mouse IgG (1:200)	Invitrogen	Cat#A21202; RRID: AB_141607
Alexa 488 rabbit anti-goat IgG (1:200)	Invitrogen	Cat#A11078; RRID: AB_141838
Alexa 594 chicken anti-goat IgG (1:200)	Invitrogen	Cat#A21468; RRID: AB_141859
Alexa 594 donkey anti-chicken IgG (1:200)	Jackson Immuno	Cat#703-585-155; RRID: AB_2340377
Alexa 594 donkey anti-mouse IgG (1:200)	Invitrogen	Cat#A21203; RRID: AB_141633
Alexa 647 donkey anti-goat IgG (1:200)	Invitrogen	Cat#A32849; RRID: AB_2762840
Chemicals, peptides, and recombinant proteins		
Recombinant murine EGF	Peprotech	Cat#31509
Recombinant mouse Noggin	R&D	Cat#1967
Recombinant mouse R-spondin1	R&D	Cat#3474-RS
A83-01	Tocris	Cat#2939
Matrigel Growth Factor Reduced	Corning	Cat#354234
N-2 supplement (100X)	Thermo Fisher	Cat#17502-048
B-27 Supplement (50X), serum free	Thermo Fisher	Cat#17504-044
Activin A	Nacalai Tesque	Cat#18585-81
CHIR99021	Cayman Chemicals	Cat#13122
Recombinant human FGF4	Peprotech	Cat#100-31
Y-27632	Fujifilm Wako Pure Chemical	Cat#253-00513
FGF-basic(154a.a.), Human, Recombinant	Peprotech	Cat#100-18B
Recombinant Human IGF-I	BioLegend	Cat#590906
Cellartis DEF-CS™ 500 culture system	Takara Bio	Cat#Y50101
Hoechst33342	Thermo Fisher	Cat#H3570
Critical commercial assays		
RNAscope 2.5HD Assay-Red	Advanced Cell Diagnostics	Cat#322350
Toray 3D-GENE™ human oligo chip 25k set	Toray Industries	N/A
RNeasy Mini kit	QIAGEN	Cat#74106
QuantiTect Reverse Transcription Kit	QIAGEN	Cat#205313

Continued

REAGENT or RESOURCE	SOURCE	IDENTIFIER
Deposited data		
Microarray data for the hindgut spheroids	This paper	GEO: GSE63473
Experimental models: Cell lines		
Human induced pluripotent stem cell line: HiPS-RIKEN-2F	RIKEN BRC Cell Bank (Japan)	HPS0014
Human induced pluripotent stem cell line: PB001	Kindly gifted by Dr Hideki Masaki (Institute of Medical Science, the University of Tokyo)	N/A
Experimental models: Organisms/strains		
NOD.Cg-$Prkdc^{scid}$/$Il2rg^{tm1wjl}$/SzJ (NSG) mice	The Jackson Laboratory Japan	N/A
Oligonucleotides		
RNAscope Probe-Hs-LGR5	Advanced Cell Diagnostics	Cat#311021
Primer: CDX2 Fwd: CTCGGCAGCCAAGTGAAAAC	This paper	N/A
Primer: CDX2 Rev: CTCCTTTGCTCTGCGGTTCT	This paper	N/A
Primer: SOX2 Fwd: GCTTAGCCTCGTCGATGAAC	This paper	N/A
Primer: SOX2 Rev: AACCCCAAGATGCACAACTC	This paper	N/A
Primer: FOXF1 Fwd: AGCAGCCGTATCTGCACCAGAA	This paper	N/A
Primer: FOXF1 Rev: CTCCTTTCGGTCACACATGCTG	This paper	N/A
Primer: Vimentin Fwd: AGGCAAAGCAGGAGTCCACTGA	This paper	N/A
Primer: Vimentin Rev: ATCTGGCGTTCCAGGGACTCAT	This paper	N/A
Primer: β-actin Fwd: GGATGCAGAAGGAGATCACTG	This paper	N/A
Primer: β-actin Rev: CGATCCACACGGAGTACTTG	This paper	N/A
Software and algorithms		
Prism 9	GraphPad	N/A
R software version 4.0.4	The R Foundation	https://www.r-project.org/
R ggplot2 package version 3.3.3	Rousselet et al.[36]	https://cran.r-project.org/web/packages/ggplot2/index.html
bootcorci package version 0.0.0.9000	Rousselet et al.[36]	https://github.com/GRousselet/bootcorci
Cell3 iMager duos Software version 1.6	SCREEN Holdings	N/A
Other		
EZSPHERE 6-well plate	AGC Inc.	Cat#4810-900SP
EZ-BindShut® 96-well plate	AGC Inc.	Cat#4870-800SP
Ultra-low attachment 6-well plate	Corning	Cat#3471
CellPet 3D-iPS system	SHIMADZU corp.	N/A
STEMFULL Centrifuge tube	Sumitomo Bakelite Co., Ltd	Cat#MS-90150
Sunflower Mini-shaker	bioSan	BS-010151-AAG
Cell3 iMager duos	SCREEN Holdings	CC-8000

RESOURCE AVAILABILITY

Lead contact
Further information and requests for resources and reagents should be directed to and will be fulfilled by the lead contact, Tomohiro Mizutani (tmizutani.gast@tmd.ac.jp).

Materials availability
This study did not generate new unique reagents.

Data and code availability
The processed gene expression data in this paper have been deposited into the NCBI Gene Expression Omnibus (GEO): GSE182230. This paper does not report original code.

Any additional information required to reanalyze the data reported in this paper is available from the lead contact upon request.

EXPERIMENTAL MODEL AND SUBJECT DETAILS

Animals

Immunocompromised nonobese diabetic severe combined immunodeficiency (NOD/SCID) interleukin-2 receptor gamma chain (IL2Rγ ^{null}) (NSG) mice, 8–9 weeks old, were used in all experiments (obtained from The Jackson Laboratory Japan, Inc.). All mice were housed in the animal facility at Tokyo Medical and Dental University. All experiments were performed with the approval of the Animal Care and Use Committee of Tokyo Medical and Dental University (A2021-225A).

Cell culture of iPSCs

The human iPSC line HiPS-RIKEN-2F was established from Japanese male umbilical cord fibroblasts and reprogrammed by retroviral expression of *Oct3/4*, *Klf4 Sox2*, and *c-Myc* (OKSM). This line was obtained from RIKEN BRC Cell Bank (Tsukuba, Japan) by kind courtesy of Dr. Yukio Nakamura (RIKEN BRC).[37] The human iPSC line PB001 was established from peripheral blood cells and reprogrammed using a Sendai virus vector expressing OKSM and was transduced by a lentiviral vector expressing tdTOMATO. PB001 was gifted by Dr. Hideki Masaki (Institute of Medical Science, the University of Tokyo).[38] Human iPSC lines were maintained in feeder-free condition using the Cellartis® DEF-CS^{TM} 500 culture system (Takara Bio) on a 6-well plate (Falcon) at 37°C in humidified air with 5% CO^2 according to the manufacturer's protocol. Confluent cells were passaged using 1x TrypLE Select Enzyme (GIBCO).

METHOD DETAILS

Differentiation of human iPSCs into intestinal spheroids

Intestinal spheroid induction was performed as described previously, with modifications.[8,9,15] Differentiation on days 0–6 was performed along with the previous publications but the process on day 6–7 was altered from the previous induction protocol. Briefly, approximately 80% confluent iPSCs were treated with 100 ng mL^{-1} activin A (Nacalai Tesque) and 3 μM CHIR99021 (Cayman Chemicals) for 1 day and 100 ng mL^{-1} activin A for the following two days. After differentiation into definitive endoderm, cells were treated with mid/hindgut differentiation medium (RMPI1640 (Sigma) with 1x L-glutamine (Nacalai Tesque), 2% Embryonic stem-cell Fetal Bovine Serum (GIBCO), 1x Penicillin-Streptomycin Mixed Solution (Nacalai Tesque) supplemented with 500 ng mL^{-1} FGF4 (Peprotech) and 3 μM CHIR99021). The medium was changed daily. Mid/hindgut floating spheroids (t-Spheroids) were present in culture media from day 6 and were collected from day 6 to day 8. For the suspension spheroid (s-Spheroid) formation, on day 6 cells were dissociated with TrypLE Select for 5 minutes at 37°C, rinsed with Advanced Dulbecco's Modified Eagle Medium/F12 (AdDMEM/F12) and centrifuged at 150 *g* for 3 minutes. Approximately 2.0 × 10^6 cells were seeded onto each well of EZSPHERE 6-well plates (4810-900SP, 4810-901SP, 4810-905SP AGC Inc.) to generate spheroids and cultured with 500 ng mL^{-1} FGF4, 3 μM CHIR99021, and 10 μM Y-27632 (Fujifilm Wako Pure Chemical) for 24 hours. As for large-size spheroid formation, 1 × 10^5 cells were seeded onto each well of the EZ-BindShut 96-well plate (4870-800SP AGC Inc.) and cultured for 24 hours. Time-lapse imaging of spheroid formation was captured using a BZ-X710 microscope (Keyence). Spheroid sizes were measured using Cell3 iMager duos (SCREEN Holdings Co., Ltd.) and analyzed with Cell3 iMager duos Software Ver. 1.6 (SCREEN Holdings Co., Ltd.). The boxplot graph of the spheroid size and seeded cell numbers was created in R using the ggplot2 package.

HIO differentiation in suspension culture

24 hours after seeding cells, subsequent spheroids were collected. EZSPHERE plates were gently shaken to allow spheroids to float out from the microwells. Spheroids should be collected quickly to prevent fusion. Supernatant containing spheroids were transferred to a low attachment 15 mL conical tube (SUMILON Stem Full; Sumitomo Bakelite) using 1,000 μL pipette. The conical tube was centrifuged at 40 *g* for 3 minutes and supernatant was discarded. Ice-cold culture medium was added to the conical tube and the spheroid suspension was transferred to ultra-low attachment 6-well plate (Corning). Culture medium composition was as follows; AdDMEM/F12 containing 10% Matrigel Growth Factor Reduced (Corning), 1x GlutaMAX (Thermo Fisher), 15 mM HEPES (Nacalai Tesque), 1x N-2 supplement (Thermo Fisher), 1x B-27 supplement (Thermo Fisher), Penicillin-Streptomycin Mixed Solution and growth factors as follows: (1) ENR containing 50 ng mL^{-1} EGF (Peprotech), 100 ng mL^{-1} Noggin (R&D) and 1,000 ng ml^{-1} R-spondin1 (R&D), (2) E(N)R containing 50 ng mL^{-1} EGF 1000 ng ml^{-1} R-spondin1 and 100 ng mL^{-1} Noggin from day 1 to day 4, and (3) E(N)RA containing 50 ng mL^{-1} EGF, 1,000 ng ml^{-1} R-spondin1, 500 nM A83-01(Tocris), and 100 ng mL^{-1} Noggin from day 1 to day 4. The medium was changed every three days. Spheroid sizes were measured using Cell3 iMager duos (SCREEN Holdings Co., Ltd.) at each time point and analyzed with Cell3 iMager duos Software Ver. 1.6 (SCREEN Holdings Co., Ltd.).

HIO differentiation in the three-dimensional culture

Traditional three-dimensional culture of spheroids was conducted according to the previously published protocols.[8,15] Briefly, spheroids were collected and embedded in Matrigel, then seeded onto 24-well culture plate (Falcon) in 30–50 μL droplets. The culture plate was then placed at 37°C for 30 minutes to polymerize the Matrigel droplet. Culture medium was added to each well, and changed every 3–4 days.

![CellPress logo] **CellPress**
OPEN ACCESS

Culture of suspension HIOs in a rotating bioreactor

After 3 days of culture in the ultra-low attachment plate, spheroids were collected and transferred to bioreactor culture vessel. When culturing large spheroids (1×10^5 cells/spheroid), less than 20 spheroids were loaded in a 10 mL culture vessel. Culture vessels were rotated on CellPet 3D-iPS system (CELLFLOAT, SHIMADZU corp.). Rotation speed started from 8 rpm with minor adjustments as spheroids grew. Medium was changed every 3–4 days.

RNA isolation and qRT-PCR

RNA was extracted using RNeasy Mini kit (Qiagen) and reverse transcribed into cDNA using QuantiTect Reverse Transcription Kit (Qiagen) according to the manufacturer's protocol. Primer sequences are listed in key resources table. qRT-PCR was performed using QuantiTect SybrGreen Master mix (Qiagen) on a StepOnePlus Real-Time PCR (Applied Biosystems). Relative expression was determined using the $\varDelta\varDelta$ Ct method and normalized to beta-actin. Statistical analysis was performed using GraphPad Prism 9.

Microarray analysis

Microarray analysis was conducted using the Toray 3D-GENE™ human oligo chip 25k set (Toray Industries). Total RNA was extracted from s-Spheroids and t-Spheroids differentiated from RIKEN-2F and PB001. Each sample was biologically triplicated. Scatter plots were visualized in R software version 4.0.4. using the ggplot2 package version 3.3.3. Correlation coefficients and comparisons were carried out using bootcorci package (ver 0.0.0.9000).[36] The acquired data were deposited in the Gene Expression Omnibus database (GEO, http://www.ncbi.nlm.nih.gov/geo/) and are accessible through the GEO Series accession number GSE182230.

Immunofluorescent staining of spheroids

Immunohistochemistry of spheroids was performed as previously described.[39] Briefly, cultured spheroids or transplanted spheroids were fixed for 2 hours in 4% paraformaldehyde (PFA) at 4°C, washed with phosphate-buffered saline (PBS), then placed in 30% sucrose buffer overnight and frozen in OCT compound. Sections were cut at 8 μm for standard microscopy, subjected to antigen retrieval, rinsed 3 times in PBS with 0.05% Tween20 (PBS-T), and blocked with blocking buffer (Blocking One, Nacalai tesque) for 1 hour at room temperature. Slides were incubated with primary antibody overnight at 4°C, washed 3 times, incubated with secondary antibody in blocking buffer for 1 hour at room temperature, washed 3 times in PBS-T. The primary and secondary antibodies employed for these assays are listed in key resources table. Tyramide signal amplification (Thermo Fisher) was used for immunofluorescent detection of CDX2, SATB2, and CA2. The slides were washed and mounted using VECTASHIELD mounting medium with DAPI (VECTOR Laboratories). Images were captured using either BZ-X710 or a laser-scanning confocal microscope (FLUOVIEW FV3000, OLYMPUS).

Immunofluorescent staining of whole-mount spheroids

Immunofluorescent staining of whole-mount spheroids was performed based on the previous tissue-clearing protocol with some modification.[40] Spheroids were fixed overnight in 4% PFA, washed with PBS, and permeabilized in PBS with 1% Triton X-100 (Sigma-Aldrich) for 6 hours at room temperature on a rocking platform. Spheroids were then incubated in primary antibody for 3 days at 4°C, washed 3 times (2 hours each) with PBS containing 0.1% Triton X-100 and 0.2% BSA at 4°C and incubated in secondary antibody for 2 days at 4°C on a rocking platform. Hoechst33342 (Thermo Fisher) was added to secondary antibody solution after 24 hour incubation. Subsequently, spheroids were washed 3 times and incubated in fructose–glycerol clearing solution (60% (vol/vol) glycerol and 2.5 M fructose) for 20 minutes at room temperature. Confocal images were captured on FV3000 and Z-stacks were analyzed and assembled using FV3000 software (OLYMPUS).

In situ hybridization

Sections of engrafted tissue used in the immunofluorescent staining were processed in hybridization steps. *In situ* hybridization was performed using an RNAscope 2.5HD Assay-Red (Advanced Cell Diagnostics) according to the manufacturer's protocols.[41] For detecting human *LGR5* expression, we used the *LGR5* RNAscope target probe (#311021) and compared it with Hs-PPIB and DapB probes as positive and negative controls, respectively.

Spheroid transplantation

Experiments were performed on female and male 8–10 weeks old NSG mice (20–24 g in weight). All mice were provided food and water *ad libitum* before and after surgeries. Spheroids were matured *in vitro* for 30 days and used for transplantation experiments. Transplantation into the mouse mesentery was performed as previously described with some modifications.[26,27] Briefly, mice were anesthetized with 2% inhaled isoflurane, and the abdominal wall was sterilized with 70% ethanol. 2 cm abdominal wall and peritoneum incision was made to gain access to the abdominal cavity. The cecum was identified and gently pulled out using a cotton swab, with the small intestine. The mesentery was spread out and HIOs were placed on the bifurcation of mesenteric vessels. Fibrin sealant

(Beriplast, CSL Behring) was applied onto the HIOs to allow for better engraftment. Subsequently, the intestines were returned to the abdominal cavity and the abdominal wall was closed using 4-0 VICRYL (ETHICON). At 4 weeks following engraftment, the recipient mice were euthanized and subjected to further experimentation.

QUANTIFICATION AND STATISTICAL ANALYSIS

All error bars indicate the SD. The quantified data represent the findings of three or more independent experiments. Statistical analyses of qRT-PCR were performed using the Prism 9 software program (GraphPad). Correlation coefficients and comparisons in microarray analyses were carried out using R software version 4.0.4. and bootcorci package (ver 0.0.0.9000).